Nanofabrication, characterization and modeling of colloidal gold nanoparticles

Introduction to nanophysics

Academic year 2019/20

Final laboratory report

Matteo De Tullio Marco Ferrari Arianna Mischianti

March 19, 2021

Contents

1 Introduction and goals of the experiment

The aim of this report is to carry out a description of the several methods adopted in order to nanofabricate, characterize and model colloidal gold nanoparticles. The analysis of the provided experimental data eventually allows to bring some improvements into the procedure. This experiment can be divided into three main steps.

- The ***first phase*** involves the nanofabrication of spherical gold nanoparticles through a synthesis obtained using the Turkevich method into an aqueous solution. Thus a Lambert-Beer-like measurement of the optical absorbance is performed in a range of frequencies that goes from the visible to the near infrared. Afterwards, a comparison is done between the experimental trend and a simulated one based on the Mie theory in dipolar approximation. The fit was performed with the χ^2 minimization method. This will allow to make a size correction to the dielectric function and extract size and concentration of the nanoparticles as well as the refractive index of the medium material.
- The goal of the ***second phase*** consists in using x-ray diffraction in Grazing Incidence geometry in order to obtain an independent measurement of the nanoparticles size. After that, it is possible to compare the results to the ones accomplished through the optical measurements.
- As final activity, in the ***third phase***, the scanning electron microscopy technique (SEM) is employed in order to perform a morpho-compositional analysis which provides the ultimate nanoparticles profile.

2 Nanofabrication and measurement of the optical absorbance

2.1 Experimental setup and procedure

The first step the Turkevic method was used to prepare an aqueous solution containing *gold* nanoparticles sized around $10 \div 20$ nm. The idea behind the procedure was about trying to

produce a supersaturated solution of gold atoms by detaching them from a suitable precursor molecule by adding a reducing agent. Then nanoparticles begin to aggregate and grow and this phase has to occur into a constant temperature environment in order to keep homogeneous and controlled the nucleation process around the liquid: the final hope is to obtain a reasonably monodispersed system.
The precursor used in the experiment was a sample of 9.5 mL of a tetrachloro-auric acid ($HAUCl_4$) solution and it was put in a baker, while the reducing agent was a solution of sodium citrate ($Na_3C_6H_5O_7$). Both solutions were heated up to 100°C, so that the boiling temperature of the water ensured the temperature to remain at a constant value during the operations. A quantity of 0.5 mL of citrate was added to the precursor to reduce the acid and free the gold atoms and it has also the benefit of creating a sort of layer around the nanoparticles, preventing them from growing too much.
During the growth period (∼15 minutes) a mechanical stirrer was activated in order to have a better homogeneous distribution of temperature and concentration of the ingredients. A remarkable fact to notice is that over this process it occurs a change of color of the solution, passing from yellow to transparent and finally turns into a dark violet shade.
The next action was to take 300 μL of the obtained solution with a micropipette and dilute it with 2700 μL of ultrapure H_2O, then save the final content in a plastic cuvette, kept at room temperature.
The final step consisted in placing the cuvette into the Jasco V670 spectrometer, which provides optical measurements, such as transmittance, which is possible to deduce the **absorbance** from.

Jasco V670 spectrometer This instrument has been employed with the aim of characterizing the optical properties of the nanoparticles. It has a chamber where the sample has to be placed, a source of light able to deliver photons from 200 up to 2700 nm in wavelength. The internal structure of this instrument is quite complicated; it is important to remark though that it has two sources of light: a *tungsten* and a *deuterium* lamp, acting respectively in VIS-NIR and UV range. The emitted photons are directed through a mirror to a grating, which provides monochromation of the light because of Bragg refraction. Finally, another mirror redirects the beam just obtained towards the mounted sample, so that the monochromatic photons pierce it orthogonally. Then Lambert-Beer-like measurements of the system are obtained as a function of the wavelength.

2.2 Data analysis

In using the Turkevic method, it is taken into account the fact that the Au nanoparticles should have a radius

$$R << \lambda$$

where λ is the wavelength of the light photons investing the sample. This allows to work within the *dipolar approximation*, where the NPs have a spherical shape and don't need to develop interactions with each other, so that we expect to obtain, at the end of the analysis, a small *filling fraction*

$$f \leq 0.1$$

i.e. the fraction of space filled by Au NPs.
In order to perform the analysis we found the Fermi velocity, the plasma frequency, and the value for the reciprocal of the mean free time between ionic collisions for the bulk Au in the book *Ashcroft, N. and Mermin, N. (1976) Solid State Physics - Harcourt Brace College Publishers, New York.* All of them are reported in table 1.

cuvette thickness [cm]	ω_P [10^{16} s^{-1}]	v_F [10^{15} $\frac{\text{nm}}{s}$]	Γ_{bulk} [10^{14} s^{-1}]
1	1.37	1.4	1.07

Table 1: Values for some parameters useful to perform the simulation. ω_P is the plasma frequency, v_F the Fermi velocity and Γ_{bulk} the relaxation frequency.

To set the simulation, some ranges has been decided for the values of radius, refractive index, and the concentration. Hence, to give us an idea of them it was performed some calculations taking into account the experimental data:

- In the case of the refractive index it wasn't just used the theoretical value:1.33. To estimate ε_m, from which it is possible to find the refractive index, we used the one obtained by applying the *Frölich condition*:
$$\varepsilon_1 + 2\varepsilon_m = 0; \tag{1}$$
that is valid in resonance conditions. So fitting a small range around the resonance peak, using a gaussian function with a first-grade polynomial (in order to taking in account the different height of the two tails of the peak), the resonance wavelength was found, and choosing from the Johnson and Christy data for the dielectric function the real part ε_1 associated the values obtained are displayed in table 2.

- To estimate the numerical density, it was taken into account that the area under the peak of all the theoretical absorbance, obtained by varying (n,R) in the chosen range, should be equal to the area under the experimental peak, in order to conserve the total mass of the NPs. So leaving ρ as a variable, a set of values of it was found, and it was realized that it varies into the order of $10^{16} - 10^{19}\text{m}^{-3}$.

χ^2	dof	λ [nm]	ϵ_1 [$\frac{\text{C}^2}{\text{N}\cdot\text{m}^2}$]	ϵ_m [$\frac{\text{C}^2}{\text{N}\cdot\text{m}^2}$]	n
0.006	169	531	-4.64	2.32	1.52

Table 2: Here are some remarkable results obtained using the Frölich condition, where ϵ_1 is the real part value of the experimental dielectric function of gold calculated at the resonance peak in wavelength, ϵ_m is the dielectric constant of the medium and n is his refractive index.

Finally it was possible to find the extinction cross section, using for the aim the dielectric function found for a thin film of Au particles by Johnson and Christy, following the formula:

$$\sigma_{ext} = 9\,\frac{\omega}{c}\,\varepsilon_m^{3/2}\,V\frac{\varepsilon_2}{(\varepsilon_1 + 2\varepsilon_m)^2 + \varepsilon_2^2} \tag{2}$$

Then the simulation of the absorbance was performed using the following equation:

$$A = \log_{10}(e)\,\gamma\,z = \log_{10}(e)\,\rho\,\sigma_{ext}\,z \tag{3}$$

with $V = \frac{4}{3}\pi R^3$ and the just found σ_{ext}.

Each simulation parameter (the radius and the density of the NPs and the refractive index of the medium) the was obtained from a set of values minimizing the χ^2 between the experimental absorbance spectrum and the simulate one. The two spectra are reported in figure 2. It was soon realized that the theory did not meet the experimental data properly.
So, to take into account the size dependence, a correction was performed to the dielectric function used, took as bulk function of Au:

$$\varepsilon(\omega, R) = \varepsilon(\omega, \infty) + \omega_P^2 \left(\frac{1}{\omega^2 - \Gamma_\infty^2} + \frac{1}{\omega^2 + \Gamma^2(R)} \right) - i \frac{\omega_P^2}{\omega} \left(\frac{\Gamma_\infty}{\omega^2 + \Gamma_\infty^2} - \frac{\Gamma(R)}{\omega^2 + \Gamma^2(R)} \right) \quad (4)$$

With $\Gamma(R)$ is the size-dependent relaxation frequency:

$$\Gamma(R) = \Gamma_\infty + \frac{\pi}{4} \frac{v_F}{R}. \quad (5)$$

In figure 1 are shown both imaginary and real part of the dielectric function and the corresponding corrected functions.
As expected, it can be seen that the two corrected parts of the dielectric function are both above the not corrected functions.
Then the same analysis was proposed to check if there was a better agreement, as it can be seen from figure 2.
The best fit parameters are reported in table 3.

	ρ [10^{18} m^{-3}]	R [nm]	n	χ^2_{min}
Not size corrected	2.12	6.16	1.46	0.0032
Size corrected	1.64	6.94	1.46	0.0006

Table 3: Here are the parameters obtained from the minimization of the absorbance χ^2 distribution with and without *size correction*. ρ is the concentration of the gold nanoparticles, R their average radius, n the refractive index of the medium containing them.

To evaluate the stability basin of the results, a contour plot of the χ^2 values was performed keeping constant one of the three parameters and letting vary the other two, as it can be seen in fig.s 3, 4, 5.

As a final check, the filling-factor was calculated to verify the independent NPs approximation is rightful:

$$f = \rho V = 2.2 \times 10^{-6}. \quad (6)$$

3 X-rays diffraction

3.1 Experimental setup and procedure

The setup used in this phase of the experiment consists in the previous solution of Au nanoparticles prepared in the first session, a substrate of silicon and an X-ray diffractometer. The procedure involves the deposition of the Au nanoparticles on the substrate in such a way that they are trapped into it forming a disordered pattern. The diffractometer provides an X-ray spectrum for the sample, which has been acquired, allowing to reconstruct that pattern and finally find the size of the nanoparticles.

3.2 Data analysis

The θ angle can be defined as the incidence diffraction angle, and appears in the Bragg law that rules the diffraction theory:

$$2\, d \sin\theta = \lambda \quad (7)$$

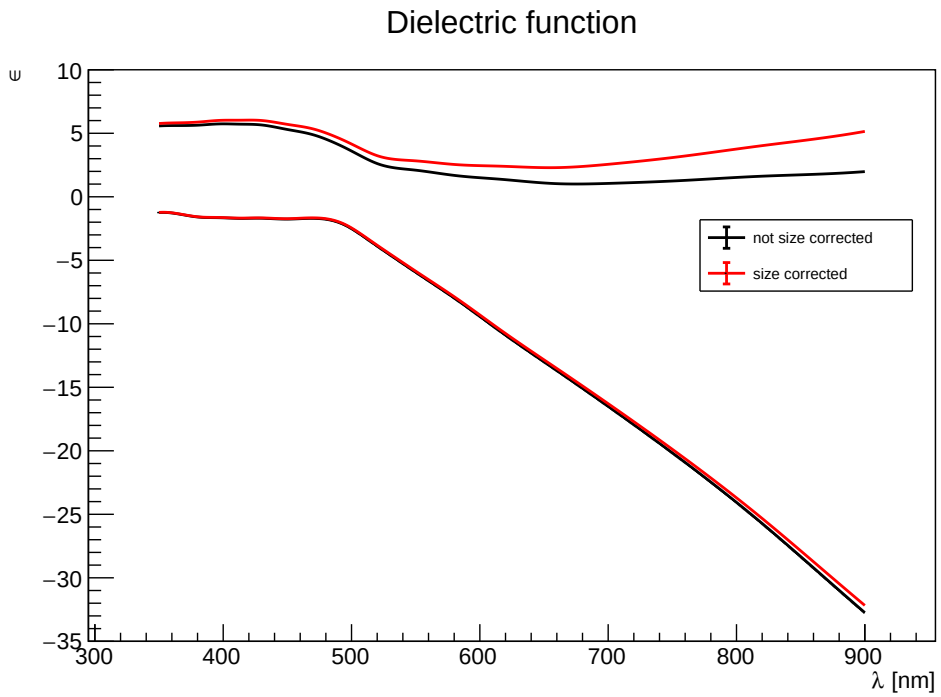

Figure 1: Comparison between experimental dielectric function of Au and the size corrected one for both its *real* and *imaginary* part.

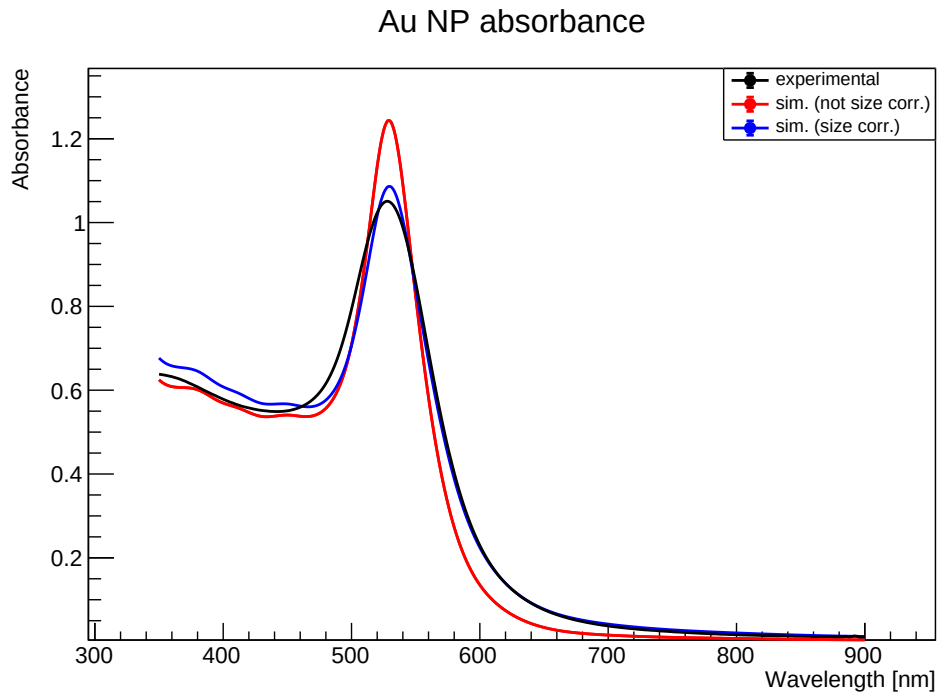

Figure 2: Here we have a comparison between the experimental absorbance and the theoretical one using the radius, the density and the dielectric constant of the medium obtained from the minimization of the χ^2 for the size corrected dielectric function and the not size corrected

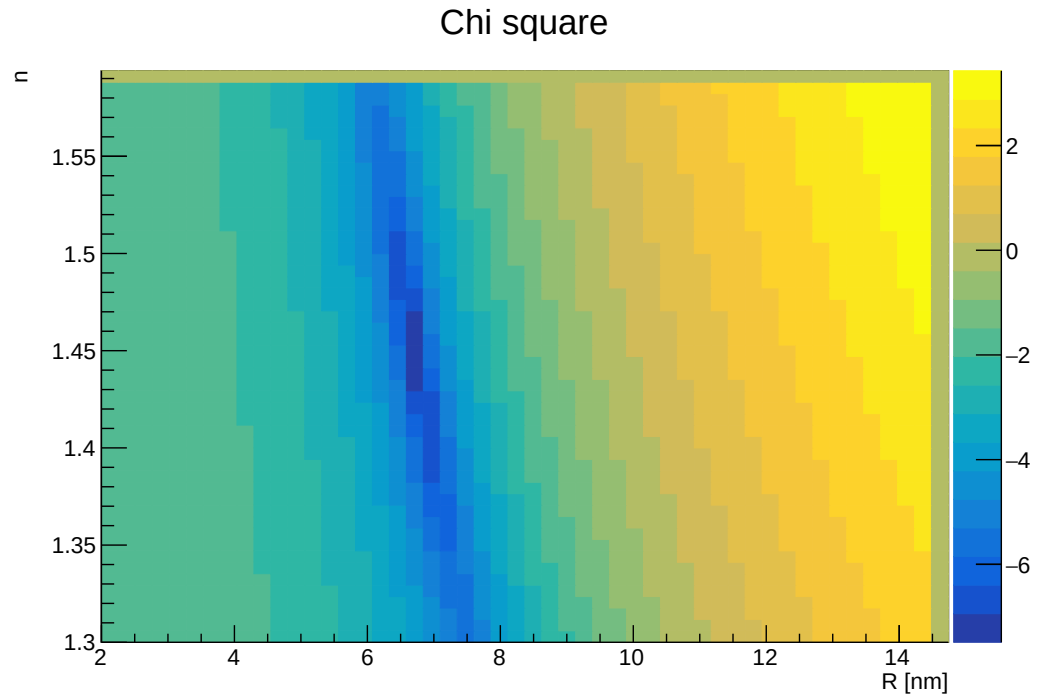

Figure 3: Contour plot of the χ^2 logarithm, with fixed density, as a function of refractive index and radius.

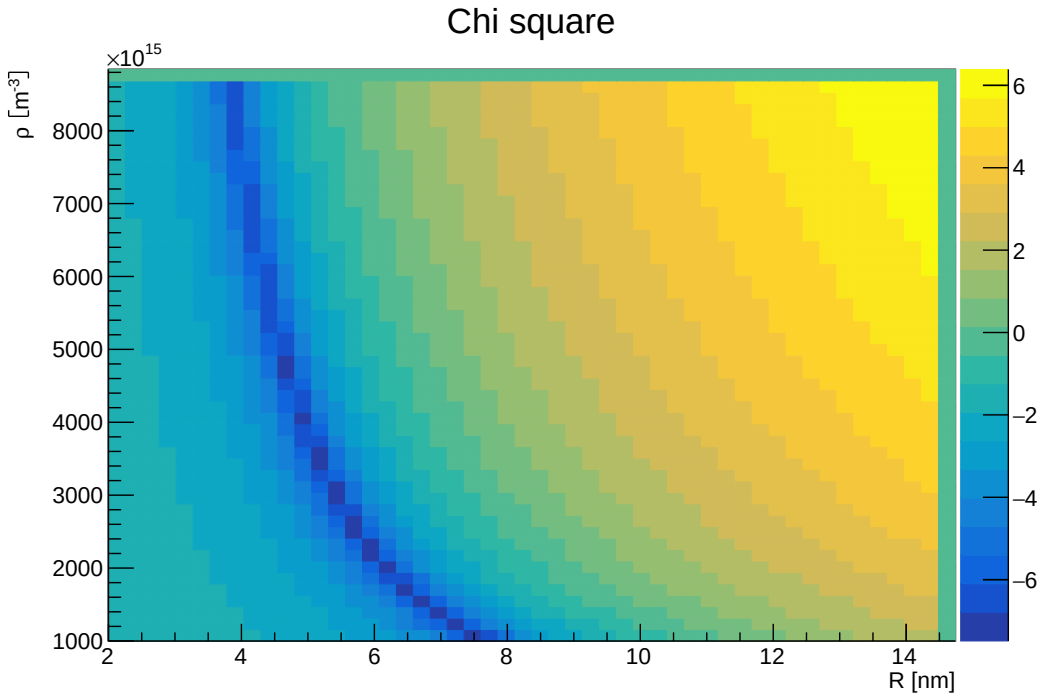

Figure 4: Contour plot of the χ^2 logarithm, with fixed refractive index, as a function of density and radius.

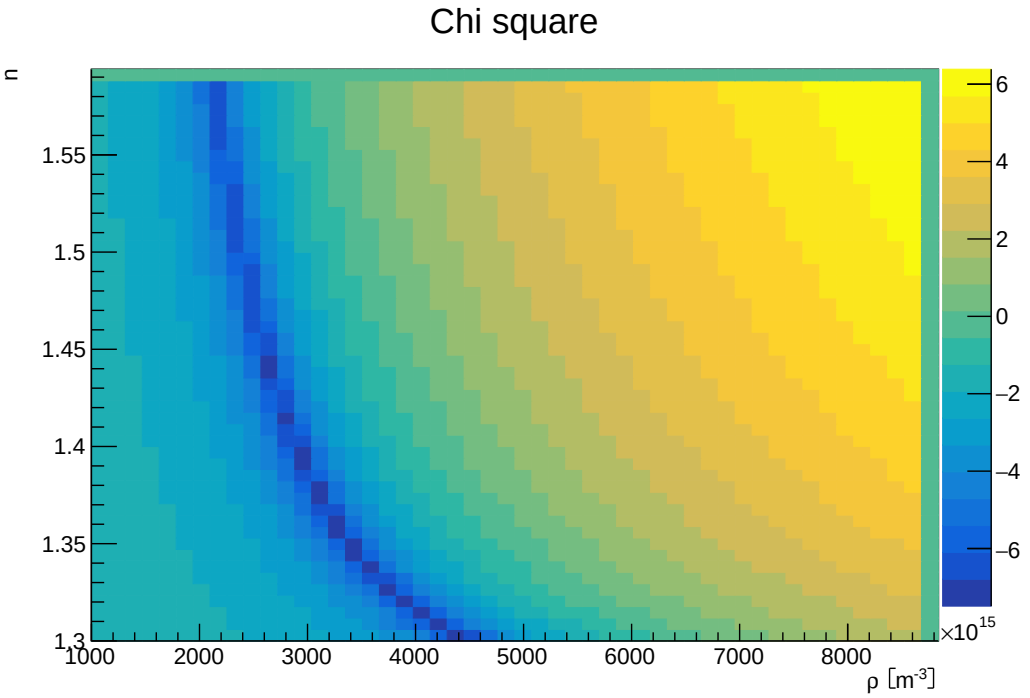

Figure 5: Contour plot of the χ^2 logarithm, with fixed radius, as a function of refractive index and density.

With the X-rays diffraction a diffused radiation was obtained between the angles

$$2\theta \in [30°,\ 90°]$$

with 2θ is the angle formed between the outgoing beam and the transmitted beam. The spectrum is reported in figure 6.
First of all the peaks were fit to find center, height and FWHM, with a Pseudo-Voigt function and a first degree polynomial to take off the noise due mainly to the Bremsstrahlung radiation and excluding the ones in the range $[50° - 60°]$ because they are related to the silicon substrate and the interest is only regarding the gold nanoparticles diffraction.
Then the Miller indexes was assigned to all peaks, taking into account that, for a FCC lattice structure, the structure factor is different from zero only if h, k, l are all even or all odd; plus, using the relation:

$$d = \frac{\lambda}{2\sin\theta} = \frac{a}{\sqrt{h^2 + k^2 + l^2}} \tag{8}$$

with a is the given lattice parameter ($a = 0.478nm$), λ is the wavelength of the incident X-ray ($\lambda^{\mathrm{Cu}}_{k\alpha_1} = 1.5406$ Å) and θ is half of the centroid of the peak took into account. In figure 6 are represented the results of this process.

Moving to the data analysis, the first step is to find the interplanar distance, in this way it is possible to estimate the lattice parameter for each peak, using again the identity 8.

Finally, using the Sherrer equation:

$$D_V = K\frac{\lambda}{\beta\,\cos\theta} \tag{9}$$

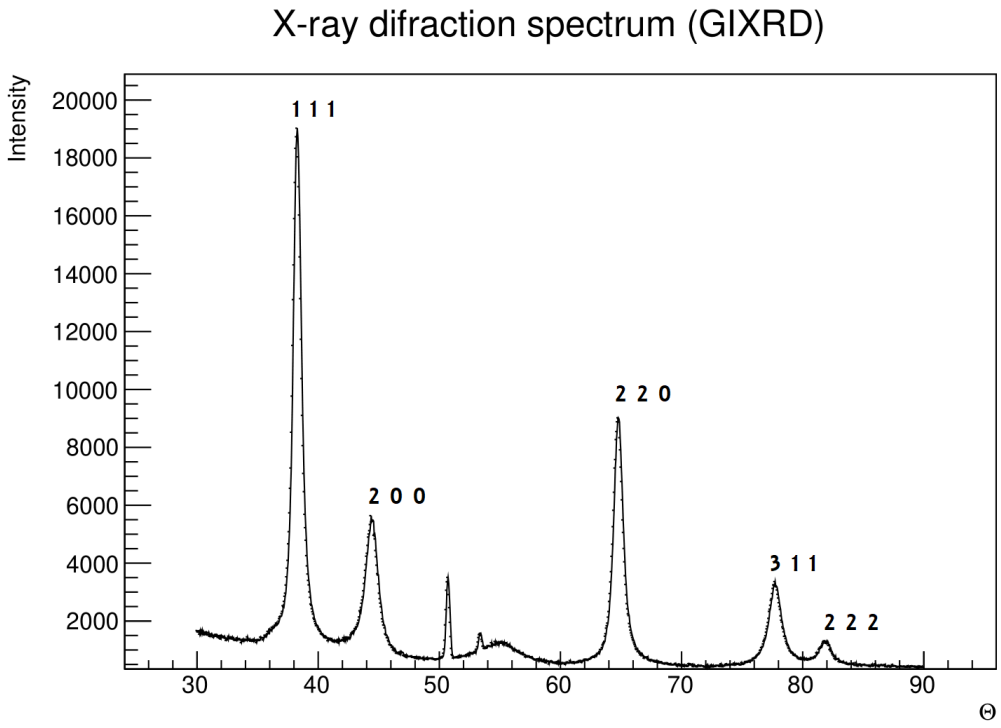

Figure 6: Peaks after the process of assigning Miller indexes.

it was possible to evaluate for each peak an estimation of the radius. This equation was found observing small crystallites and bonds the cristallite size D_V volume weighted, to the broadening β made by two contributions, β_{obs} is the FWHM of the peaks, β_{instr} is related to the sperimental apparatus and they are connected by the following formula:

$$\beta = \sqrt{\beta_{obs}^2 - \beta_{instr}^2} \tag{10}$$

K is the Scherrer constant that since it was used the FWHM way to find β, it assumes the value 0.89.
Hence, the clusters were consituted by one crystallite, so D could be interpreted as the diameter of the nanoparticle. In tab. 4 are shown all the remarkable results: interplanar distance, lattice parameter, and the radius from each peak of the diffraction spectrum. Noticing that for the radius the values are so dispersed, we have chosen to take as best estimate the one corresponding to the first diffraction peak, which is the one with higher statistics.
Notice also that we have assumed a negligible strain contribution to the broadening of the GIXRD peaks. This hypothesis was investigated and the results discussed in the section 5.

4 Scanning Electron Microscopy

4.1 Experimental setup and procedure

A Scanning Electron Microscopy (SEM) system was used in order to perform the analysis of the morphological composition of the nanoparticles. In particular this technique has been employed to obtain a direct measurement of their dimensions and to map their shape more accurately. The microscope emits an electronic beam, which excites the electrons in the more external shells of the Au atoms in the nanoparticles. Then the electrons experience a de-excitation leading

Peak	Miller indexes (h,k,l)	Centroid 2θ [deg]	FWHM [deg] [deg]	Lattice constant a [Å]	Radius R [nm]
1	(1,1,1)	38.29 ± 0.01	0.791 ± 0.004	4.0684 ± 0.0001	5.5952 ± 0.0003
2	(2,0,0)	44.41 ± 0.01	1.266 ± 0.009	4.0765 ± 0.0002	3.4307 ± 0.0006
3	(2,2,0)	64.80 ± 0.01	0.917 ± 0.006	4.0661 ± 0.0001	5.3099 ± 0.0011
4	(3,1,1)	77.73 ± 0.01	1.252 ± 0.016	4.0717 ± 0.0001	4.1279 ± 0.0040
5	(2,2,2)	81.94 ± 0.02	2.048 ± 0.016	4.0698 ± 0.0001	2.5620 ± 0.0101

Table 4: Parameters obtained from data analysis of X-ray diffraction session. Errors are evaluated as the square root of the sum of the single variable relative errors squared.

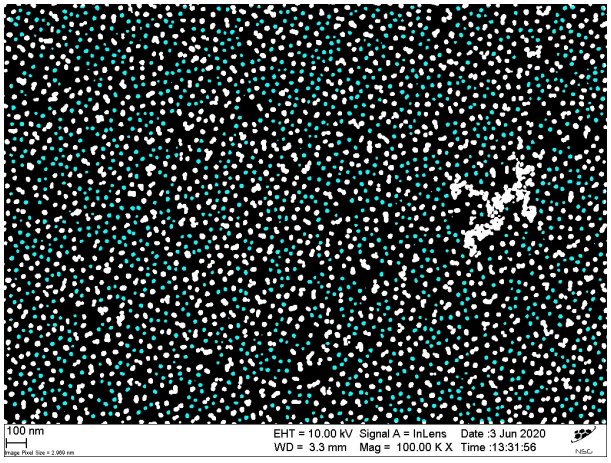

(a) Processing Au NPs. We can easily distinguish wide clusters, such as the one on the right, which will be neglected in the following.

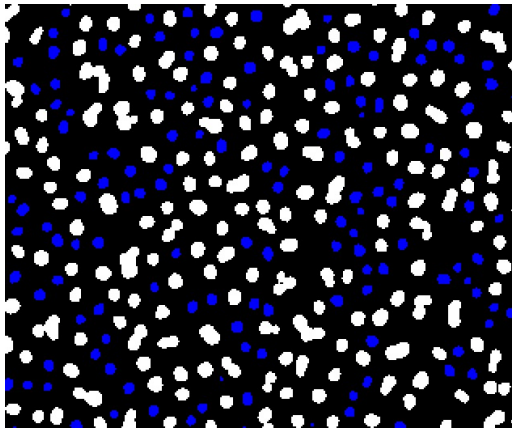

(b) Result of cropping figure 7a: in blue are the particles selected for our analysis.

Figure 7: NPs analysis on ImageJ.

them to lower energy states, with a consequent emission of X-rays characterized by a specific wavelength range. Finally, by using the software ImageJ we were able to obtain again another measurement for the radius of the Au nanoparticles to compare to the ones found in the previous sessions.

4.2 Data analysis

The first step of the analysis was to edit the images provided by the SEM technique through the software ImageJ. In figure (7b) it is possible to observe two possible scenarios as a result of the deposition process: clusters and isolated nanoparticles. Our job was to apply a filter to pick the ones characterized by some specific features needed. In particular we chose a range of *areas* between 25 and 800 nm^2 and set for the *circularity* parameter values between 0.8 and 1 (the closer to 1 the more circular is the nanoparticle). In doing so, we attempted to neglect some wide clusters and ellipsoidal nanoparticles (which are, in most cases, a result of the superposition of two or more circular nanoparticles). Moreover, the choice of the circularity range is especially relevant, as the software is not able to distinguish an isolated nanoparticle from an overlapped one. Clearly these constraints lead to have a poorer statistic, but we still managed to deal with a sufficient number of particles, enough to obtain a decent estimate for their average radius.
Once selected the group of nanoparticles we are interested in, it was possible to extract some data for each one. For instance, the software provided their area: by simply assuming that they

are perfectly circular we were able to extract their radius. After having collected all the radii we managed to arrange them into an histogram. Hence, in order to find the average radius we fitted it using a *LogNormal distribution*, as it was the best adapted-curve to our statistic. The results taken from ImageJ are shown in figure 8. To have a confirmation of our result we also calculated a second estimate of the average radius by performing the average of the nanoparticles volumes and then obtaining the radius from it. The software also provided the axes of the nanoparticles (which are actually elliptical), and by using them we were able to evaluate their *eccentricity* taking into account the expression:

$$e = \sqrt{1 - \left(\frac{a_2}{a_1}\right)^2} \tag{11}$$

where obviously $a_1 > a_2 = a_3$ (a_3 is the semiaxis in the third dimension). Clearly the analysis was carried out in 2D, so we only needed a_1 and a_2. Then we put the single-particle eccentricities into and histogram and fitted it with a Gaussian to finally calculate the average eccentricity, as shown in figure 9. The numerical results are reported in table 5.

# of used NPs	**Minimum radius**	**Maximum radius**	**Average radius**	**Volume-averaged radius**	**Average eccentricity**
N	R_{min} [nm]	R_{max} [nm]	$\langle R \rangle$ [nm]	$\langle R^3 \rangle^{\frac{1}{3}}$ [nm]	e
2330	2.9	15.9	10.9 ± 2.2	11.4 ± 0.7	0.513 ± 0.003

Table 5: List of some useful parameters obtained by analyzing data provided by the software ImageJ.

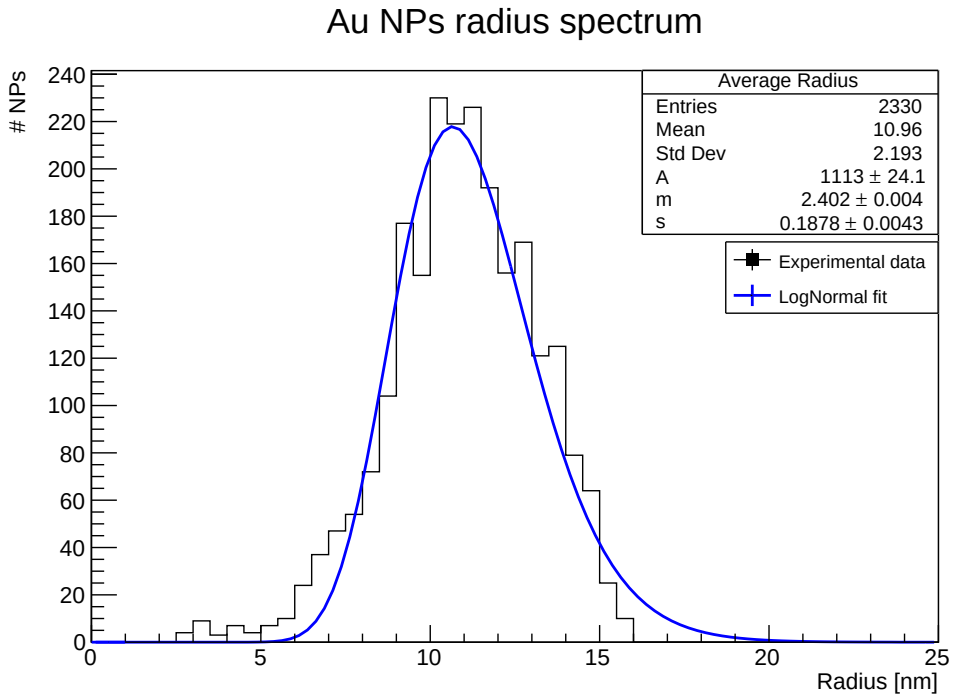

Figure 8: Histogram collecting the nanoparticles radii. We managed to fit with a *LogNormal distribution* to obtain the average value $\langle R \rangle$, which is reported in table 5.

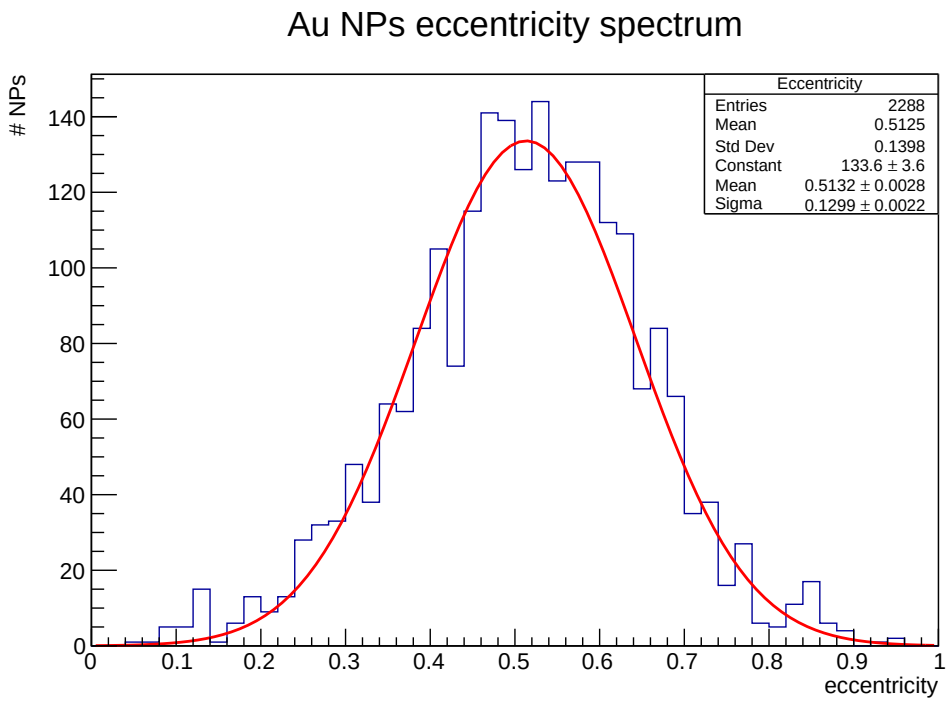

Figure 9: Histogram for the eccentricity values of the selected nanoparticles. It has been fitted using a gaussian in order to find the *average* eccentricity value, which is reported in table 5.

5 Results and improvements

The three values for the radius are shown in table 6.

Experiment	R [nm]
Absorbtion spectrum	6.94
X-ray diffraction	5.59
SEM	10.95

Table 6: Here are the different Radius values for each kind of analysis.

As it can be seen there is an incompatibility between the indirect methods of measurement and the direct one. The SEM analysis is the direct analysis because it allows to measure directly the diameter of the nanoparticles, so it can be taken as the best extimation of the radius. The other two indirect methods can be affected by the shape of the nanoparcticles, their internal structure, the kind of matrix that surrounds them, etc. The first thing to say is that a check from the X-ray analysis done with the SEM shows that the composition of the nanoparticles was just gold, so we can exclude that the clusters were made by other elements in addition to Au.

To understand why there is this difference it was decided to try to correct the two indirect methods of measurements.
For the X-ray diffraction analysis one of the assumption made was the particles were made by just one crystallite, but since the particles could be made by more than one of them, what we measured as radius of the nanoparticle could be actually the radius of crystallites composing

the clusters.
For strained or imperfect crystals it is needed to take into account a different line broadening, using the Williamson-Hall relationship:

$$(\beta_{obs} - \beta_{instr})\,\cos\theta = K\frac{\lambda}{D_V} + 4\,\epsilon_{strain}\,\sin\theta \tag{12}$$

from the plot it was obtained the following fit in fig.10, and from the fit parameters it is possible

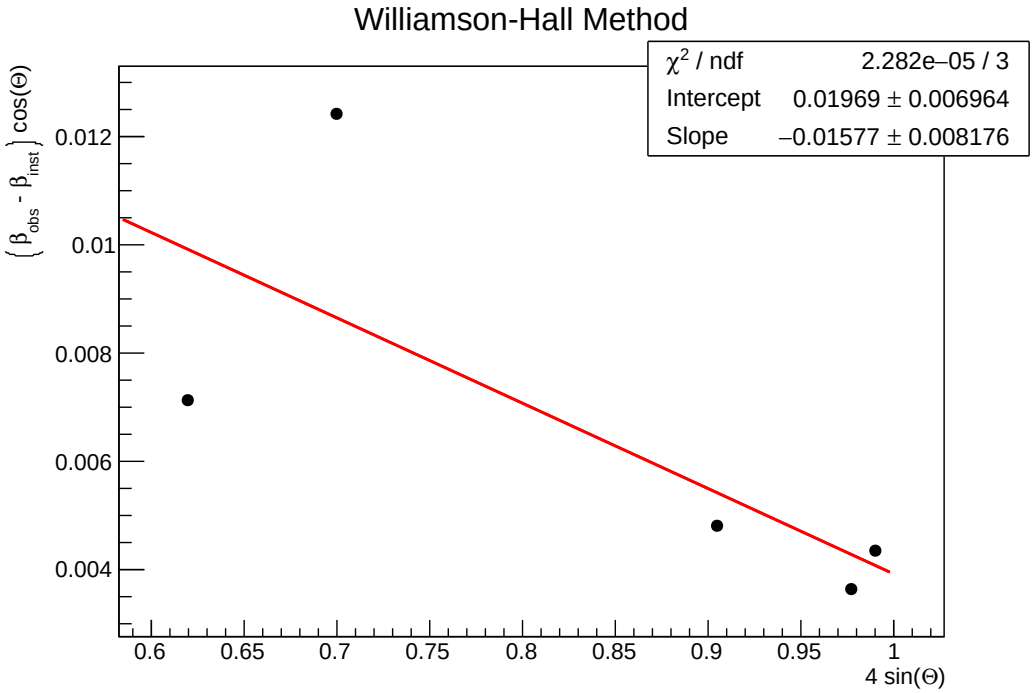

Figure 10: Williamson-Hall fit. On the Y-axis $(\beta_{obs} - \beta_{instr})\cos\theta$ values are plotted while, on the X-axis, $4sin\theta$ values. The strain is obtainable from the slope parameter, and the intercept is $K\frac{\lambda}{D_V}$, which is possible to find a new value of the radius from.

to derive a new value for the radius

$$R = 3.48\,\text{nm}$$

and a value for the strain of

$$\epsilon_{strain} = -0.016$$

Clearly this is not the way to recover the damage, actually the radius value get worse and the strain is small and negative, so not particularly influent, so this analysis was useless.
For the absobance spectrum the assumptions are the dipolar approximation, and so the fact that the radius of the nanoparticles had to be small, spherical and they had to be quite distant one from the others. The filling factor was computed so the independence on the nanoparticles is already confirmed. The small radius hypotesis is again confirmed, because in the SEM analysis it was found for the biggest nanoparticle a radius of 15.895nm, which is ok to be considered small.
The only thing that can be discussed is the circularity of the nanoparticles: from the SEM analysis it is quite obvious that this is not satisfied. So a remake of all the computations was tried with the Gans theory for elliptical nanoparticles, that put a correction in the extiction

cross section:

$$\sigma_{ext} = \frac{1}{3}\frac{\omega}{c}\varepsilon_m^{3/2} V \sum_{j=1}^{3}\left[\frac{\varepsilon_2/L_j^2}{\left(\varepsilon_1 + \varepsilon_m\left(\frac{1-L_j}{L_j}\right)\right)^2 + \varepsilon_2^2}\right] \tag{13}$$

whith:

$$L_1 = \frac{1-e^2}{e^2}\left[\frac{1}{2e}\ln\left(\frac{1+e}{1-e}\right) - 1\right]; \quad L_2 = L_3 = \frac{1-L_1}{2}. \tag{14}$$

And as a consequence also the Frolich condition is changed:

$$\sum_{j=1}^{3}\left(\varepsilon_1 + \varepsilon_m\frac{1-L_j}{L_j}\right) = 0. \tag{15}$$

The refractive index calculated from the resonance condition of the Gans extinction cross section is $n = 1.51$, it is still high with respect to the one of pure water, even if smaller than the one calculated with the Frolich condition for spherical particles, wich is highly an overestimation of the theoretical one (1.33).
With applying this theory, new values for the density, the radius and ε_m are found using the χ^2 method, that are reported in the first line of table 7.

	ε_m	n	ρ [10^{17} m^{-3}]	R [nm]	χ^2
R as a variable parameter	2.07	1.44	1.288	8.5	$5.14{\cdot}10^{-4}$
R fixed at 10.9 nm	1.94	1.39	0.694	10.9	$1.44{\cdot}10^{-3}$

Table 7: In this table is reported a comparison between the results obtained by a minimization of the χ^2 within Gans theory in the two cases of the radius as free or fixed parameter.

It seems that the refractive index is the closer one to the one expected, and a bigger value of the radius has been found, the closer one to the one of the SEM and it can be seen from the χ^2 value and fig. 11 that this is actually the best representation of the data. Even if there is still a redshift of the peak with respect to the experimental data. To give us an idea of what happen if the SEM value is used to fix the radius parameter, the fit was done again keeping fix the radius value.
The curve shown in figure 12 is not a good extimation of the curve (see the χ^2 value with respect to the other χ^2 values, however is still small) but is the less red-shifted curve of all the fits, and also the best value for the refractive index is indeed obtained, as it can be seen in tab. 7, so everything seems to go in the right direction if the radius is the one obtained with the SEM analysis.

6 Conclusions

By using these three methods of studying gold nanoparticles, the differences between a direct and an indirect method are understandable: a direct method allows to experience the nanoscale world by visualizing directly the nanoparticles, leading us to comprehend the differences from

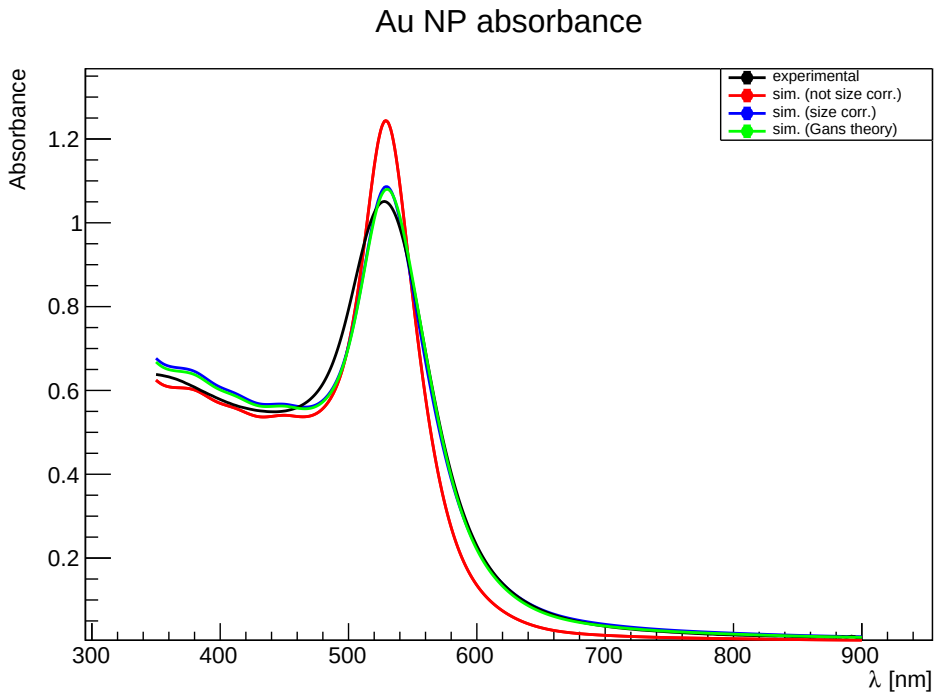

Figure 11: Absorbtion spectrum of Gans theory compared to the other theories and the experimental data.

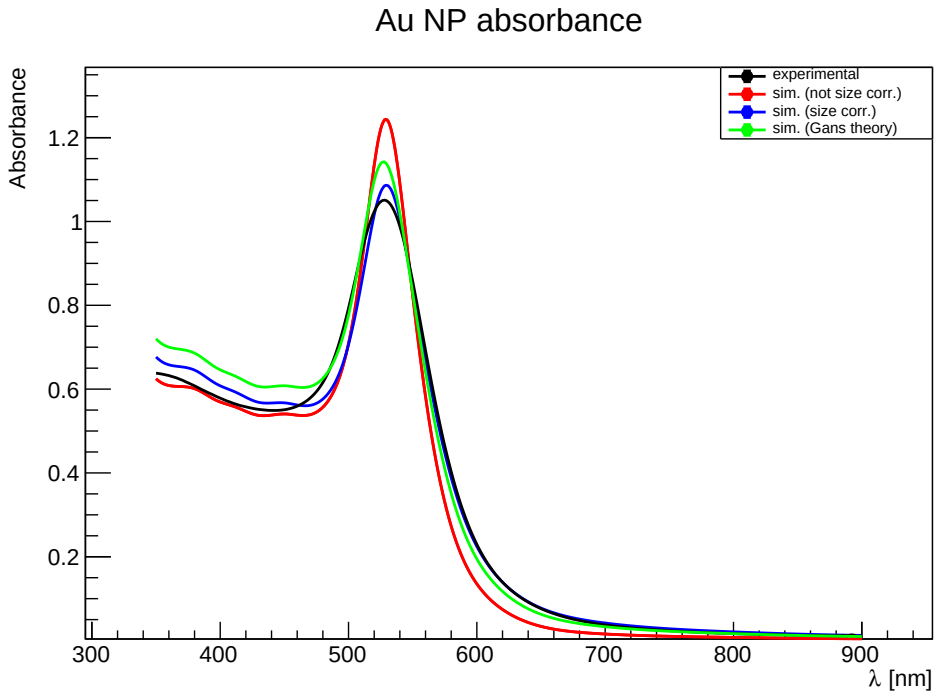

Figure 12: Absorbtion spectrum of Gans theory with radius fixed compared to the other theories and the experimental data.

the theory and the real life such as finding different shapes, or the distance between the particles. Also it was possible to select the NPs, to better estimate the distribution of the radii, so, to take as the best value for the radius the one from the SEM analysis, is a reliable choice.

Using the theory studied from the course lessons, it was performed the best data analysis that we were able to do, applying where possible some corrections.
Finally, keeping the radius fixed at 10.9 nm, the one from the SEM, it was possible to see actually that the centroid of the peak is the one that corresponds the best with the experimental one, which may confirm the assumptions made.